FINITE-STATE AEROELASTIC MODELLING OF MORPHING WING THROUGH UNSTEADY LIFTING-LINE THEORY

Riccardo Giansante[1], Giovanni Bernardini[1] & Massimo Gennaretti[1]

[1]Department of Civil, Computer Science and Aeronautical Technologies Engineering, Via della Vasca Navale, 79, Rome, Italy, 00146

Abstract

A state-space formulation for the study of the aeroelastic behavior of morphing wings is presented. It is based on an Unsteady Lifting-Line Theory model for the prediction of the aerodynamic loads coupled with a structural dynamics model to obtain an aeroelastic operator suitable for stability analysis and aeroservoelastic applications. The sectional unsteady aerodynamic loads are evaluated by the application of the Küssner-Schwarz theory, with wake inflow from trailed vorticity determined numerically application of the Biot-Savart law. The wake vorticity release derives from the evaluation of the sectional bound circulation given by the Kutta-Joukowski theorem extended to unsteady flows. The accuracy of the overall aeroelastic model is assessed by comparison with experimental data regarding the paper flutter phenomenon considered in the literature. The results from the proposed model present a good correlation with the experimental data, and highlight the important role of the trailed vorticity.

Keywords: unsteady aerodynamics, aeroelasticity, state-space, lifting-line theory, morphing wings

1. Introduction

Since the beginning of aviation engineers have tried to develop the best aircraft configurations for the wide range of purposes they were built to accomplish. Usually, conventional aircraft are optimized for a single design point: for instance, civil aircraft are built with long spans to increase efficiency, military ones with smaller swept-back wings to improve maneuverability, VTOL (vertical take-off and landing) configurations were born to operate in urban or extreme environments. However, as aeronautical technology advances, this concept is becoming more and more limiting.

As already happened in the past, engineers have drawn inspiration from nature for the definition of new paradigms of aviation. Observing the flight behavior of birds and insects shows how quickly they can change shape to move from efficient cruising conditions to agile and precise maneuvers. This extreme adaptability inspired the idea of morphing aircraft. Nevertheless, morphing is not a completely new concept. For instance, the Wright Brothers designed their Flyer including an actuating cable that could be directly controlled by the pilot to change (to morph) the twist of the wing, performing roll control. Even the classical high lift devices that we are used to seeing in the common civil aircraft, such as flaps and slats, are applied to morph the wing geometry, being deployed when needed to increase the lift by increasing the wing surface, and then retracted during the cruise phase to reduce the drag and, thus, fuel consumption.

The most comprehensive definition of "morphing" is "real-time adaptability to enable multi-point optimized performance", provided by the NATO RTO technical team in [1]. There are many different approaches regarding morphing aircraft, meticulously reviewed by Barbarino et al. [2] and more recently by Ajaj et al. [3], who divided them into three main categories of shape morphing wings: planform, out-of-plane and airfoil morphing. The planform category is divided into span, sweep and chord morphing. The out-of-plane one is achieved by the twist, the dihedral or gull and the spanwise bending. There are also two different ways of morphing the airfoil, namely through the thickness and the camber. The most widely used category is the camber morphing, due to its effectiveness and versatility.

The literature is rich in contributions regarding camber morphing. For instance, Campanile and Anders [4] have developed the belt-rib airfoil, which consists of a closed shell reinforced by hinged stiffeners, which allow in-plane deformations and whose shape can be modified through shape memory alloys or piezoelectric materials. Similarly, Woods et al. [5, 6, 7] developed the Fishbone Active Camber (FishBAC), a biologically inspired compliant airfoil in which an internal bending beam acts as a spine and an elastomeric matrix composite acts as the skin surface. A low-fidelity aeroelastic model of the FishBAC has been developed by Zhang et al. [8], which can be used for preliminary and conceptual design, as well as for optimization purposes. Murua et al. [9] (extending the work made by Palacios and Cesnik [10, 11]) developed an aeroelastic two-dimensional, multi-dofs model, examining the effect of the stiffeners on the aeroelastic stability. Drazumeric et al. [12] proposed a flexible airfoil model accomplished by the combination of a rigid airfoil-shaped leading edge, with a flexible composite thin laminated plate attached to its trailing edge. Following [9], Sambenedetto et al. presented a new aeroelastic model [13] where both rigid-body and deformable-camber degrees of freedom of a semi-infinite thin plate are considered, with control action obtained through the actuation of two piezoelectric thin foils applied to the main structure.

Aeroelastic problems related to airfoil camber deformation are studied also in fields far from aeronautics. Among them, an interesting medical application concerns the study of the aeroelastic instability of the human soft palate modelled as a flexible cantilevered plate, which occurs in the upper-airway disorder generating the condition of snoring (see [14, 15]). In addition, Watanabe et al. developed an aeroelastic model applied to the study of paper flutter [16], which is a phenomenon limiting the speed of printing in paper machines (see also [17] where an analytical state-space aeroelastic model has been developed and applied to the same problem for stability analysis and flutter control purposes), whereas flag flutter instability was examined by Argentina et al. [18] and Eloy et al. [19] (in both cases, the structural problem is modelled through a semi-infinite flexible cantilever plate).

The present paper aims to develop an aeroelastic solver for morphing wings where the aerodynamic solution is determined by an Unsteady Lifting-Line Theory, ULLT, formulation based on the Küssner-Schwarz theory [20, 21], which can be considered as the extension to deformable airfoils of the well-known Theodorsen theory [22]. In the proposed approach, the influence of the wake is considered semi-analytically: the shed vorticity effects are accounted for analytically through the Küssner-Schwarz theory, whereas the wake inflow due to trailed vortices (three-dimensional effects) is determined numerically as part of the ULLT solution process. The aeroelastic formulation developed here couples the ULLT model presented and validated in [23] with the structural dynamics operator representing a morphing wing with deformable camber, thus providing a solution tool that combines a good level of accuracy with low computational cost, making it particularly suitable for pre-design and optimization purposes.

The paper is structured as follows. First, the mathematical formulation of the unsteady aerodynamic Küssner-Schwarz theory for airfoils is briefly outlined. Then, the ULLT is recalled, along with the methodology applied to obtain the finite-state aerodynamic operator to be combined with the structural dynamics model to define the state-space aeroelastic operator suitable for stability analysis and control purposes. The accuracy of the ULLT aerodynamic solver and an analytical simplified version of it is assessed by comparison with the results given by a higher-fidelity model, and then the aeroelastic predictions concerning paper flutter are correlated with experimental data.

2. Küssner-Schwarz's Theory

The Küssner-Schwarz theory is a linear aerodynamic theory, for incompressible, potential flows providing the airfoil pressure loads generated by an arbitrary distribution of downwash [20, 21].

Let us consider a coordinate system, (x,z), with the origin located at the mid-point of an airfoil of length $2b$, the x-axis aligned with the unperturbed flow of velocity V and the airfoil, positive from the leading to the trailing edge, and the z-axis positive upward.

For $\xi = x/b = \cos\theta$, the Küssner-Schwarz theory demonstrates that, for an arbitrary downwash distribution, $v(\xi, t)$, such that, in the frequency domain,

$$\tilde{v}(\theta) = -V\left[\tilde{P}_0 + 2\sum_{n=1}^{\infty}\tilde{P}_n\cos(n\theta)\right] \tag{1}$$

with

$$\tilde{P}_n = -\frac{1}{\pi V}\int_0^{\pi}\tilde{v}(\theta)\cos(n\theta)\,\mathrm{d}\theta \tag{2}$$

the following pressure jump across the airfoil arises

$$\Delta\tilde{p}(\theta) = -\rho V^2\left[2\tilde{a}_0\tan\left(\frac{\theta}{2}\right) + 4\sum_{n=1}^{\infty}\tilde{a}_n\sin(n\theta)\right] \tag{3}$$

where ρ is the air density and $\tilde{a}_n$ are coefficients given by

$$\begin{cases}\tilde{a}_0 = C(k)(\tilde{P}_0 + \tilde{P}_1) - \tilde{P}_1 \\ \tilde{a}_n = \tilde{P}_n + ik\,(\tilde{P}_{n-1} - \tilde{P}_{n+1})/(2n) \qquad \text{for } n \geq 1\end{cases} \tag{4}$$

with the reduced frequency defined as $k = \omega b/V$ (ω is the angular frequency) and $C(k)$ representing the lift deficiency function which is defined by the Theodorsen theory [22].
For a harmonically varying camber deformation expressed as

$$Z(\xi, t) = Z_0(\xi)\,e^{i[\omega t + \phi(\xi)]} \tag{5}$$

where $\phi(\xi)$ and $Z_0(\xi)$ denote, respectively, the local angular phase and local amplitude of the deformation, the downwash is defined as follows

$$v(\xi, t) = \frac{V}{b}\frac{\partial Z}{\partial \xi} + \frac{\partial Z}{\partial t} \tag{6}$$

from which a direct relation between structural dofs and pressure jump can be easily derived.

3. Unsteady Lifting-Line Theory for Morphing Wings Aeroelasticity

In this work, the aeroelastic operator for morphing wings is derived by applying a frequency-domain Unsteady Lifting Line Theory, ULLT, solver suitable for the analysis of unsteady aerodynamics of morphing wings with deformable camber. It applies the Küssner-Schwarz theory to evaluate the pressure distribution along the whole wing, which is then integrated to obtain the generalized loads as projections onto the shape functions, ψ_j, of the distributed pressure, namely

$$f_j = -b\int_{-1}^{1}\Delta\tilde{p}(\xi)\,\psi_j(\xi)\,\mathrm{d}\xi \tag{7}$$

Given a distribution of the wake trailed vorticity, the Biot-Savart law is used to determine its effects on the sectional downwash appearing in the Küssner-Schwarz theory (which, on the other hand, already considers shed vorticity effects). A similar approach is used in [23] as an extension of the ULLT for non-morphing wings presented in [24]).
The wake vorticity released by the lifting body is determined from the relation between the sectional bound circulation and the sectional circulatory lift provided by the extension of the Kutta-Joukowski theorem to unsteady linear aerodynamics presented in [25], which closes the loop of the aerodynamic system.
This aerodynamic solution approach yields the following relation between the M generalized aerodynamic forces, $\mathbf{f}$, and the M Lagrangian coordinates, $\mathbf{q}$, of the structural dynamics problem

$$\tilde{\mathbf{f}} = \mathbf{E}(k)\,\tilde{\mathbf{q}} \tag{8}$$

where $\mathbf{E}$ is the transcendental $[M \times M]$ aerodynamic matrix, that collects the aerodynamic frequency response functions (see [23] and [24] for details).
The presence of the transcendental contributions comes from three sources: $i)$ the exponential contribution due to the delays appearing in the Biot-Savart law used to evaluate the downwash generated by the wake trailed vorticity (the vorticity at a given wake point corresponds to the vorticity released by the trailing edge when passing at that point), $ii)$ the Theodorsen's lift deficiency function used to evaluate the coefficients a_n of the Küssner-Schwarz theory (see Eq. (4)), and $iii)$ the frequency response function, $G(k)$, of the unsteady Kutta-Joukowski theorem (see [25]). This implies that, in this form, the aerodynamic matrix is unsuitable for aeroelastic stability analyses and control applications. To overcome this difficulty, it is convenient to apply the following rational-matrix approximation of the aerodynamic matrix along the imaginary axis of the complex plane

$$\mathbf{E}(k) \cong (ik)^2\mathbf{A}_2 + ik\mathbf{A}_1 + \mathbf{A}_0 + \mathbf{Q}(ik\mathbf{I} - \mathbf{A})^{-1}\mathbf{R} \tag{9}$$

where $\mathbf{A}_2$, $\mathbf{A}_1$ and $\mathbf{A}_0$ are $[M \times M]$ matrices, $\mathbf{A}$ is a diagonal $[N_p \times N_p]$ matrix, where N_p is the number of aerodynamic poles that can be arbitrarily increased to better approximate the aerodynamic transfer functions, whereas $\mathbf{Q}$ is a $[M \times N_p]$ matrix and $\mathbf{R}$ is a $[N_p \times M]$ matrix. All these constant-coefficient matrices can be determined by a least-square approximation technique [26, 13].
Thus, the combination of Eq. (9) with (8), followed by the transformation into time domain yields, for $\tau = tV/b$,

$$\begin{cases} \mathbf{f}(\tau) = \mathbf{A}_2\,\ddot{\mathbf{q}} + \mathbf{A}_1\,\dot{\mathbf{q}} + \mathbf{A}_0\,\mathbf{q} + \mathbf{Q}\,\mathbf{r} \\ \dot{\mathbf{r}} = \mathbf{A}\,\mathbf{r} + \mathbf{R}\,\mathbf{q} \end{cases} \tag{10}$$

which represents the state-space model of the wing generalized aerodynamic loads derived from the frequency-domain ULLT solver, perfectly suitable for aeroelastic stability analyses and control purposes once coupled with the operator representing the structural dynamics of the examined wing. In Eq. (10), $\mathbf{r}$ denotes the vector of the N_p additional aerodynamic states introduced by the rational contribution in Eq. (9).

3.1 Validation of the Frequency-Domain ULLT for Morphing Wings

In the following, the ULLT model is validated by comparing its unsteady loads predictions with those given by a higher-fidelity aerodynamic model. The latter consists of a zero-th order Boundary Element Method (BEM) tool based on a boundary integral equation solution for velocity potential flows, with collocation points located at the centers of the boundary discretization elements, and pressure loads evaluated through the Bernoulli theorem [27, 28, 29].
The test case analyzed is an untwisted rectangular morphing wing with chord length $c = 1$ m, span length $l = 20$ m and sweep angle $\Lambda = 30°$. The undisturbed-flow dynamic pressure is assumed to be equal to unity. The magnitude and phase of the aerodynamic matrix components are evaluated within the reduced frequency range $k \in [0, 2]$.
The set of shape functions considered for the evaluation of the generalized forces is such that they represent a wing modelled as a clamped-free bending-torsion beam, with chordwise deformation described by the eigenfunctions of a free-free uniform bending beam. Overall, four shape functions are considered, the first two corresponding to the first bending and torsion natural modes of vibration of a clamped-free rigid-section beam, and the other two consisting of the combination of the first bending mode with chordwise deformation described by the first two bending modes of the free-free beam. Therefore the aerodynamic matrix $\mathbf{E}(k)$ has dimension $[4 \times 4]$. For the sake of brevity, only 4 out of the resulting 16 transfer functions are shown. Specifically, we consider $E_{13}(k)$, which is the transfer function between the first mode of camber deformation and the generalized force related to the first wing bending mode, and $E_{34}(k)$ and $E_{43}(k)$, which are the transfer functions involving only the camber deformation modes.
These results are shown in Figs. 1 to 3. Overall, the ULLT results are in good agreement with the BEM results for the whole reduced frequency range considered, in terms of both magnitude and phase of the transfer functions. It is worth noting that the ULLT solver is significantly faster computationally than the BEM tool (it is about 2.5 times faster than the BEM).

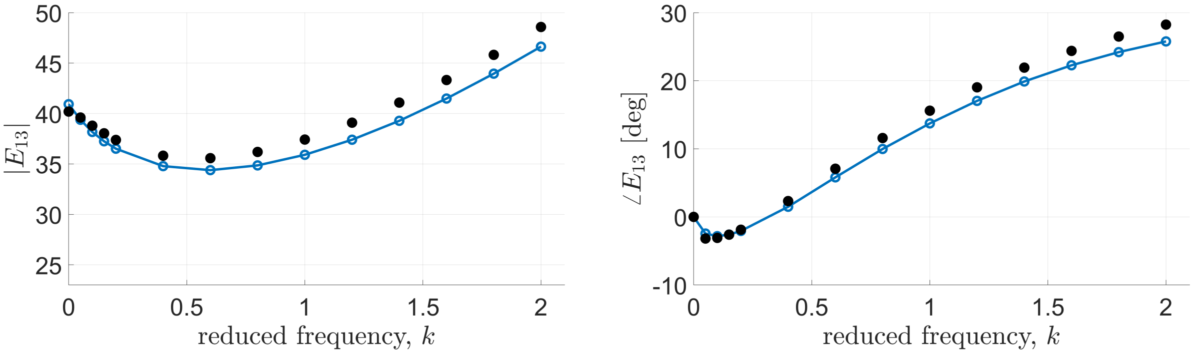

Figure 1 – Transfer function $E_{13}(k)$, blue ULLT, black BEM.

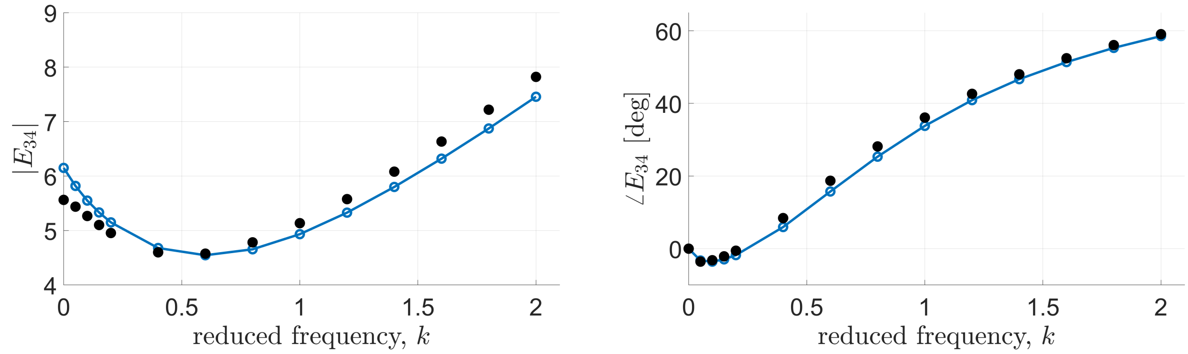

Figure 2 – Transfer function $E_{34}(k)$, blue ULLT, black BEM.

Finally, the rational matrix approximation of matrix $\mathbf{E}$ defined is performed in order to derive a reduced-order model of the aerodynamic operator to be coupled with a structural dynamics model to define the state-space aeroelastic operator. The comparisons between the transfer functions directly given by the ULLT model and those provided by the 3-pole rational-matrix approximation are shown in Figs. 4 to 6. These results show the excellent accuracy of the reduced-order model from which state-space aeroelastic operator can be readily derived.

4. Numerical Aeroelastic Investigations

This section presents some results concerning the paper flutter analysis. As already mentioned in the Introduction, it is an aeroelastic phenomenon that has been deeply investigated in the literature, from both the numerical and experimental point of view.

The present numerical results are compared with the numerical and experimental outcomes presented in [16] and [14]. Specifically, Watanabe et al. [16] developed an aeroelastic model based on the Küssner-Schwarz theory and the application of the exact transcendental form of the lift deficiency function. The velocity and frequency of paper flutter were determined through the widely-known V-g method. Instead, the experimental flutter data are provided by Watanabe et al. [16] for a wide range of paper-like materials, and by Huang for aluminum foils [14].

In the present work, the paper foils are structurally considered as semi-infinite thin plates, clamped on the side impinged by the freestream and free on the opposite side. Then, the aeroelastic system is completed by the inclusion of the aerodynamic operator, defined in two different ways. The first one consists of a fully-2D aerodynamic model based on the Küssner-Schwarz theory and developed in [17]. It considers the rational approximation of the lift deficiency function provided by Venkatesan and Friedmann [30], which allows the direct description of the aerodynamic operator in a state-space form. The second one is the ULLT model described in Section 3, which can be considered as an extension of the fully-2D model that accounts for trailed vorticity effects. In the following, the two aerodynamic models are referred to as "2D aero" and "ULLT", respectively.

Not included in the Küssner-Schwarz theory, viscous effects are introduced by superposition in both

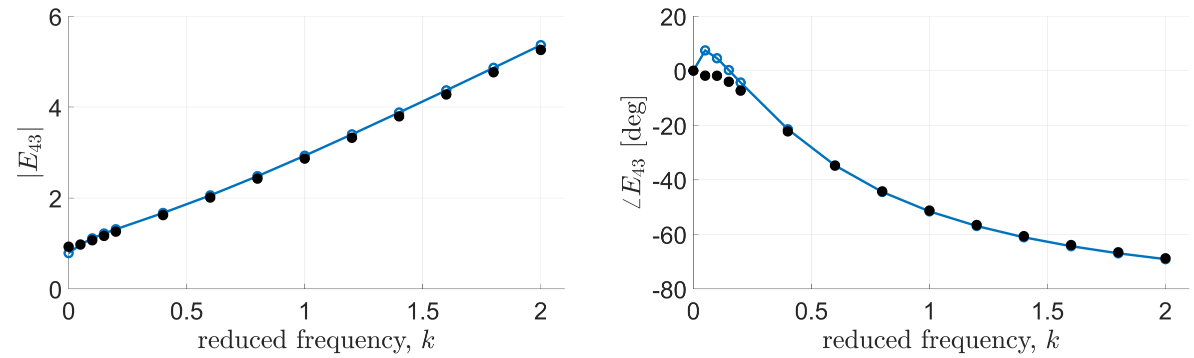

Figure 3 – Transfer function $E_{43}(k)$, blue ULLT, black BEM.

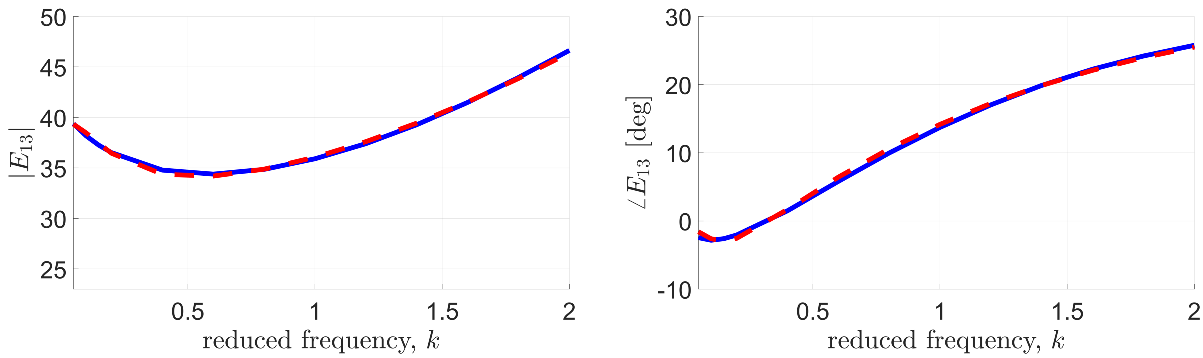

Figure 4 – RMA of the transfer function $E_{13}(k)$, blue exact, red approximated.

aerodynamic models, in order to take into account the corresponding tension loads that play a non-negligible role in this aeroelastic stability problem. This is accomplished by considering a constant viscous drag coefficient, C_d, related to the interaction between plate and fluid.

4.1 Aeroelastic Analyses through the Fully-2D Aerodynamic Model

First, the aeroelastic results obtained by the application of the fully-2D model are compared with the numerical outcomes provided by Watanabe et al. [16] for a paper of composite material (for details, see [16]).

This is shown in Fig. 7, where the nondimensional flutter velocity, U_f^*, is depicted as a function of the mass ratio, a, for three different values of the drag coefficient (present results are related to converged values of the number of natural modes of vibration, M, and the number of coefficients of the Küssner-Schwarz theory, N). Both the nondimensional flutter velocity and mass ratio are defined by Watanabe et al. as

$$U_f^* = \frac{U_f}{\sqrt{\dfrac{E_p J_p}{\rho c^3}}} \qquad , \qquad a = \frac{\rho_p t_p}{\rho c} \tag{11}$$

where U_f is the dimensional flutter velocity, $c = 2b$ is the chord, while the subscript p stands for the properties of the plate, respectively the density, ρ_p, the thickness, t_p, the Young modulus, E_p, and the moment of inertia, J_p.

Since the mass ratio is inversely proportional to the chord, the drag decreases as a increases, namely as the surface of the plate shrinks. This effect has a negative impact on the stability of the system, since the drag produces a tension stiffening the plate, thus making it more stable. Indeed, Fig. 7 shows that at low values of the mass ratio the flutter velocity increases as C_d increases. Overall, the present fully-2D model provides flutter predictions that are in perfect agreement with those by Watanabe et al. [16].

The two models show very similar results also regarding the flutter frequency, F_f, whose trend is shown in Fig. 8, where F_1, F_2, F_3, F_4 are the first four frequencies of vibration. The flutter frequency

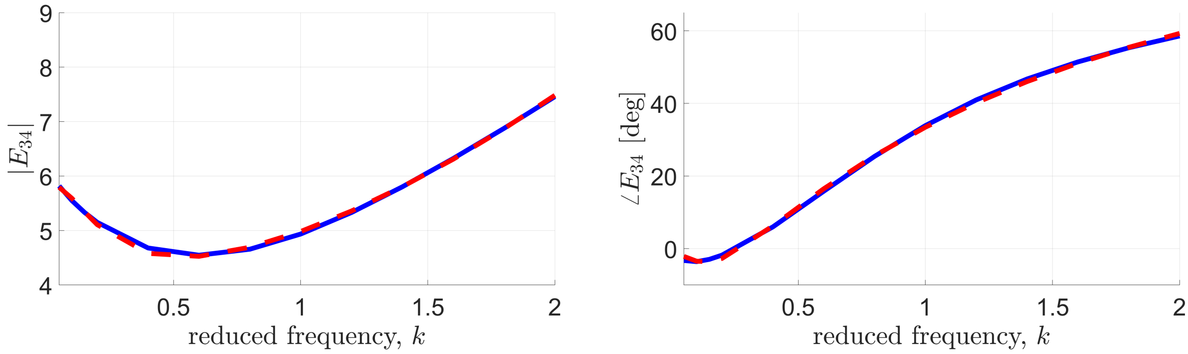

Figure 5 – RMA of the transfer function $E_{34}(k)$, blue exact, red approximated.

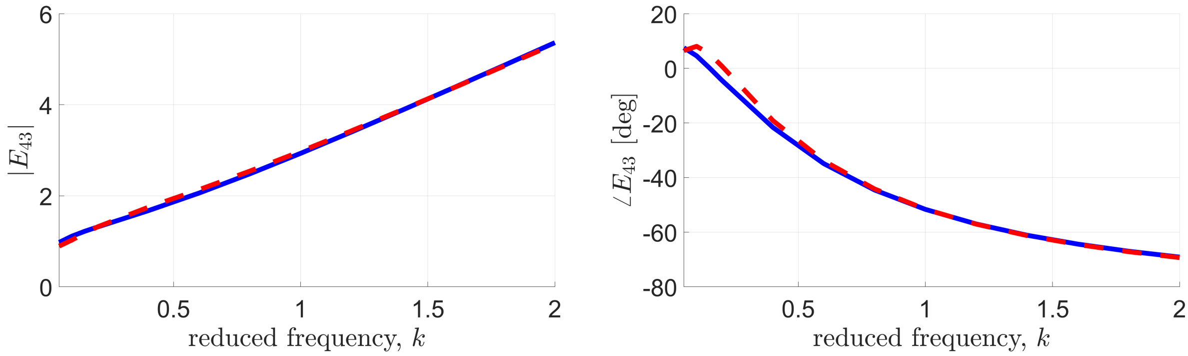

Figure 6 – RMA of the transfer function $E_{43}(k)$, blue exact, red approximated.

is strongly dependent on the mass ratio. At low mass ratios (long plates) the value of the flutter frequency tends to the natural frequency of the third mode of vibration, while at high mass ratios (small plates) it tends to the frequency of the second mode of vibration. For mid-values of a, the value of the flutter frequency is between F_2 and F_3, thus proving that the second and third natural modes of vibration are aeroelastically coupled.

Next, we compare the outcomes provided by the fully-2D model with the experimental data proposed by Watanabe et al. [16] and by Huang [14]. These results, given in terms of nondimensional flutter velocity as a function of the mass ratio, are shown in Fig. 9 for $C_d = 0.2$ and Poisson ratio equal to $\nu = 0.4$. The tension due to drag has a positive effect on the accuracy of flutter velocity predictions which are in fair agreement with the experimental data even for low values of the mass ratio (compare with Fig. 7).

4.2 Aeroelastic Analyses through the ULLT Model for Camber Morphing Wings

In Fig. 9 some discrepancies between the 2D numerical results and the experimental data appear. Here, we assess the paper flutter prediction accuracy when the ULLT model is applied, thus including the trailed vorticity effects.

In particular, we examine the problem described in [14] where an aluminum plate of span length equal to 6 cm is considered. Four different values of mass ratio are considered, corresponding to the chord lengths equal to $4, 6, 8, 10$ cm.

The results are depicted in Fig. 10 and demonstrate that the inclusion of the trailed vorticity effects in the ULLT model improves the accuracy of the flutter numerical predictions given by the fully-2D computational tool that can be considered of overall good quality.

5. Conclusions

A state-space model for the aeroelastic study of camber morphing wings is presented. The aerodynamic operator is obtained through an unsteady lifting-line theory approach based on the Küssner-Schwarz theory for the evaluation of the sectional loads. The circulatory lift of each wing section is

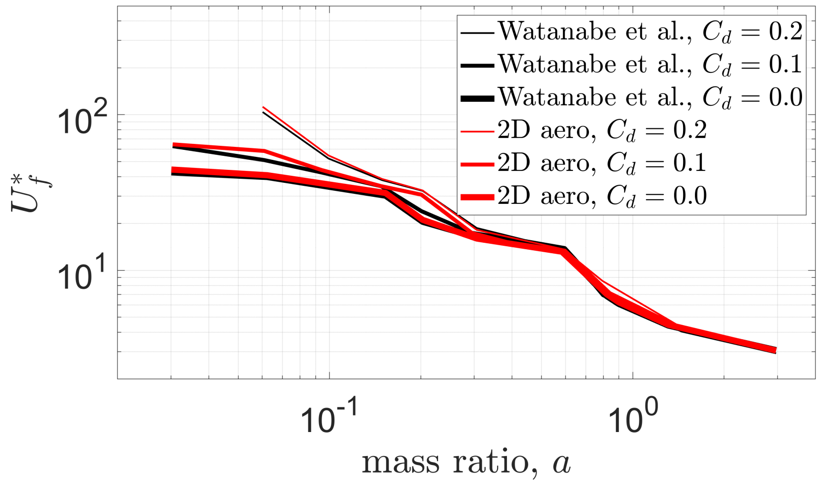

Figure 7 – Flutter velocity as a function of the mass ratio. Comparison between present results and numerical results by Watanabe et. al [16] for three different values of C_d.

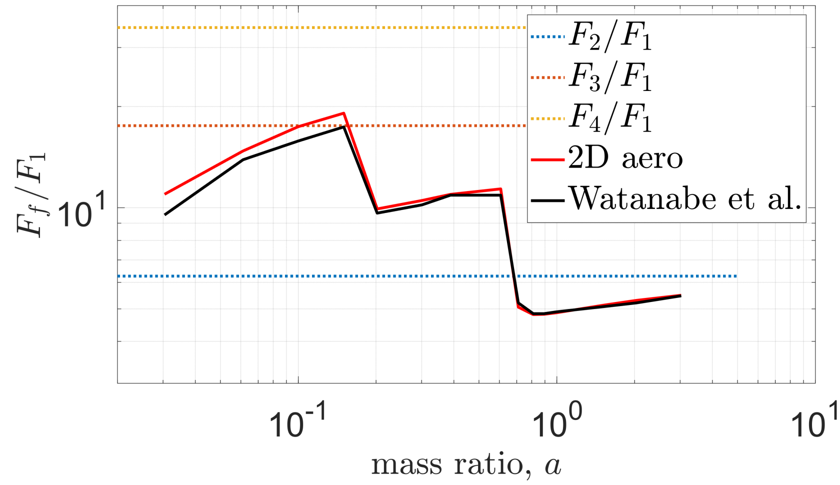

Figure 8 – Flutter frequency as a function of the mass ratio. Comparison between present results and numerical results by Watanabe et. al [16] for $C_d = 0.0$.

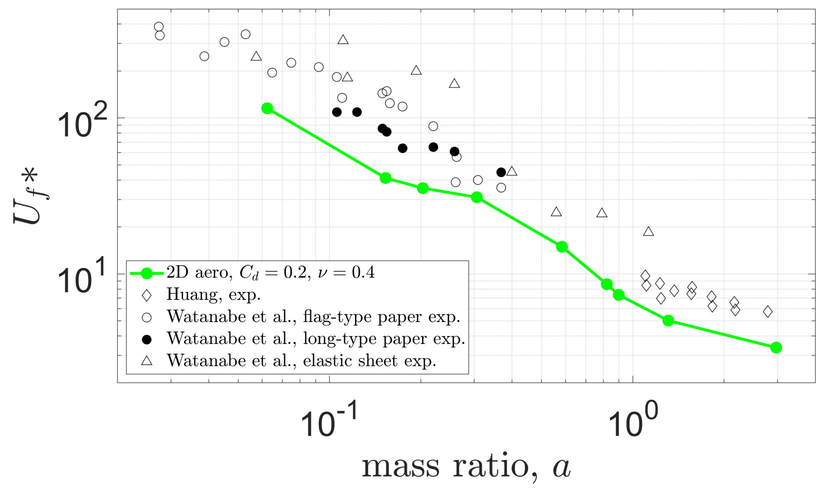

Figure 9 – Flutter velocity as a function of the mass ratio. Comparison between present results and experimental results by Watanabe et. al [16] and Huang [14] for $C_d = 0.2$ and $\nu = 0.4$.

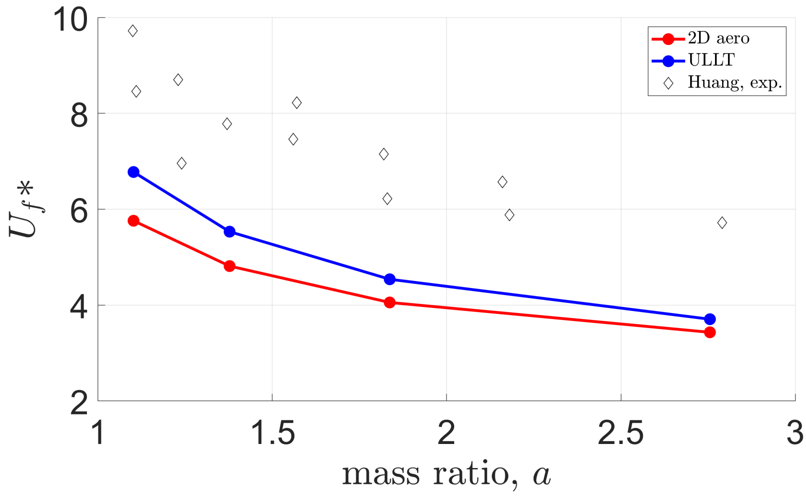

Figure 10 – Flutter velocity as a function of the mass ratio. Comparison between fully-2D present results, ULLT present results and the experimental data by Huang [14] for $C_d = 0.2$.

related to the bound circulation through an extended version of the Kutta-Joukowski theorem which is valid for unsteady linear aerodynamics. The effects of the corresponding trailed vorticity released in the wake are numerically taken into account by application of the Biot-Savart law. For a camber-deforming bending-torsion wing, the accuracy of the aerodynamic model is successfully assessed by comparing the evaluated transfer functions relating generalized forces to Lagrangian coordinates with those given by a high-fidelity computational tool. Considering the paper flutter problem, the aeroelastic model is obtained by coupling the rational-matrix approximation of the ULLT aerodynamic matrix with the structural model describing a clamped-free semi-infinite thin plate. It is demonstrated that the paper flutter velocity predictions given by the proposed state-space ULLT-based model are in good agreement with the available experimental data. It improves the results obtained by a fully-2D model still based on the Küssner-Schwarz theory, and previously validated against numerical outcomes available in the literature, which does not consider trailed vorticity effects.

6. Contact Author Email Address

riccardo.giansante@uniroma3.it

7. Copyright Statement

References

[1] McGowan AMR, Vicroy DD, Busan RC, and Hahn AS. Perspectives on highly adaptive or morphing aircraft. *Proc NATO RTO AVT-168 Symposium*, Lisbon, Portugal, No. RTO-MP-AVT-168, 2009.

[2] Barbarino S, Bilgen O, Ajaj RM, Friswell MI, and Inman DJ. A review of morphing aircraft. *Journal of Intelligent Material Systems and Structures*, Vol. 22, No. 9, pp 823–877, 2011.

[3] Ajaj RM, Parancheerivilakkathil MS, Amoozgar M, Friswell MI, and Cantwell WJ. Recent developments in the aeroelasticity of morphing aircraft. *Progress in Aerospace Sciences*, Vol. 120, pp 100682, 2021.

[4] Campanile LF and Anders S. Aerodynamic and aeroelastic amplification in adaptive belt-rib airfoils. *Aerospace Science and Technology*, Vol. 9, No. 1, pp 55–63, 2005.

[5] Woods BKS and Friswell MI. Preliminary investigation of a fishbone active camber concept. *Proc ASME 2012 Conference on Smart Materials, Adaptive Structures and Intelligent Systems*, Stone Mountain, Georgia, USA, Vol. 2, SMASIS2012-8058, pp 555-563, 2012.

[6] Woods BKS, Bilgen O, and Friswell MI. Wind tunnel testing of the fish bone active camber morphing concept. *Journal of Intelligent Material Systems and Structures*, Vol. 25, No. 7, pp 772–785, 2014.

[7] Woods BKS, Dayyani I, and Friswell MI. Fluid/structure-interaction analysis of the Fish-Bone-Active-Camber Morphing Concept. *Journal of Aircraft*, Vol. 52, No. 1, pp 307-319, 2015.

[8] Zhang J, Shaw AD, Wang C, Gu H, Amoozgar M, Friswell MI, and Woods BKS. Aeroelastic model and analysis of an active camber morphing wing. *Aerospace Science and Technology*, Vol. 111, pp 106534, 2021.

[9] Murua J, Palacios R, and Graham J. Applications of the unsteady vortex-lattice method in aircraft aeroelasticity and flight dynamics. *Progress in Aerospace Sciences*, Vol. 55, pp 46–72, 2012.

[10] Palacios R and Cesnik CES. On the one-dimensional modeling of camber bending deformations in active anisotropic slender structures. *International Journal of Solids and Structures*, Vol. 45, No. 7, pp 2097–2116, 2008.

[11] Palacios R and Cesnik CES. Low-speed aeroelastic modeling of very flexible slender wings with deformable airfoils. *Proc 49th AIAA/ASME/ASCE/AHS/ASC Structures, Structural Dynamics, and Materials Conference, 16th AIAA/ASME/AHS Adaptive Structures Conference, 10th AIAA Non-Deterministic Approaches Conference, 9th AIAA Gossamer Spacecraft Forum, 4th AIAA Multidisciplinary Design Optimization Specialists Conference*, 2008.

[12] Drazumeric R, Gjerek B, Kosel F, and Marzocca P. On bimodal flutter behavior of a flexible airfoil. *Journal of Fluids and Structures*, Vol. 45, pp 164–179, 2014.

[13] Sambenedetto E, Giansante R, Bernardini G, and Gennaretti M. A state-space aeroservoelastic model for deformable airfoils. *Proc Online Symposium on Aeroelasticity, Fluid-Structure Interaction, and Vibrations*, pp 184–191, 2021.

[14] Huang L. Flutter of cantilevered plates in axial flow. *Journal of Fluids and Structures*, Vol. 9, No. 2, pp 127–147, 1995.

[15] Balint TS and Lucey AD. Instability of a cantilevered flexible plate in viscous channel flow. *Journal of Fluids and Structures*, Vol. 20, No. 7, pp 893–912, 2005.

[16] Watanabe Y, Isogai K, Suzuki S, and Sugihara M. A theoretical study of paper flutter. *Journal of Fluids and Structures*, Vol. 16, No. 4, pp 543–560, 2002.

[17] Pisani S. Aeroservoelasticità di piastre semi-infinite tramite la teoria di küssner-schwarz. Master's thesis dissertation, Università degli Studi Roma Tre, Italy, 2023.

[18] Argentina M and Mahadevan L. Fluid-flow-induced flutter of a flag. *Proceedings of the National Academy of Sciences of the United States of America*, Vol. 102, pp 1829–34, 03 2005.

[19] Eloy C, Souilliez C, and Schouveiler L. Flutter of a rectangular plate. *Journal of Fluids and Structures*, Vol. 23, No. 6, pp 904–919, 2007.

[20] Küssner HG and Schwarz I. *The oscillating wing with aerodynamically balanced elevator*. NACA TR-991, 1941.

[21] Fung YC. *An Introduction to the Theory of Aeroelasticity*. Dover Publications, Inc., New York, 1993.

[22] Theodorsen T. *General theory of aerodynamic instability and the mechanism of flutter*. NACA TR-496, 1935.

[23] Giansante R, Bernardini G, and Gennaretti M. State-Space Lifting Line Aerodynamic Modelling for Aeroelasticity of Camber Morphing Wings. *Proc AIAA AVIATION 2023 Forum*, San Diego, CA and Online, AIAA 2023-3372, 2023.

[24] Giansante R, Bernardini G, and Gennaretti M. Frequency-domain lifting-line aerodynamic modelling for wing aeroelasticity. *Applied Sciences*, Vol. 12, No. 23, 2022.

[25] Gennaretti M and Giansante R. Kutta-Joukowski theorem for unsteady linear aerodynamics. *AIAA Journal*, Vol. 60, No. 10, pp 5779–5790, 2022.

[26] Gori R, Serafini J, Molica Colella M, and Gennaretti M. Assessment of a state-space aeroelastic rotor model for rotorcraft flight dynamics. *CEAS Aeronautical Journal*, Vol. 7, No. 3, pp 405–418, 2016.

[27] Morino L and Gennaretti M. Boundary integral equation methods for aerodynamics. *Computational Nonlinear Mechanics in Aerospace Engineering*, Progress in Astronautics and Aeronautics Series, Vol. 146, ed: Atluri SN, AIAA, Washington, DC, pp 279–320, 1992.

[28] Gennaretti M and Bernardini G. Novel boundary integral formulation for blade-vortex interaction aerodynamics of helicopter rotors. *AIAA Journal*, Vol. 45, No. 6, pp 1169–1176, 2007.

[29] Gennaretti M, Bernardini G, Serafini J, and Romani G. Rotorcraft comprehensive code assessment for blade-vortex interaction conditions. *Aerospace Science and Technology*, Vol. 80, pp 232–246, 2018.

[30] Venkatesan C and Friedmann PP. New approach to finite-state modeling of unsteady aerodynamics. *AIAA Journal*, Vol. 24, No. 12, pp 1889–1897, 1986.